Conditions that Stabilize Membrane Domains Also Antagonize *n*-Alcohol Anesthesia

Benjamin B. Machta,[1] Ellyn Gray,[2] Mariam Nouri,[2] Nicola L. C. McCarthy,[4] Erin M. Gray,[2] Ann L. Miller,[3] Nicholas J. Brooks,[4] and Sarah L. Veatch[2,*]

[1]Lewis Sigler Institute, Princeton University, Princeton, New Jersey; [2]Department of Biophysics and [3]Department of Molecular, Cellular, and Developmental Biology, University of Michigan, Ann Arbor, Michigan; and [4]Department of Chemistry, Imperial College London, South Kensington Campus, London, United Kingdom

ABSTRACT Diverse molecules induce general anesthesia with potency strongly correlated with both their hydrophobicity and their effects on certain ion channels. We recently observed that several *n*-alcohol anesthetics inhibit heterogeneity in plasma-membrane-derived vesicles by lowering the critical temperature (T_c) for phase separation. Here, we exploit conditions that stabilize membrane heterogeneity to further test the correlation between the anesthetic potency of *n*-alcohols and effects on T_c. First, we show that hexadecanol acts oppositely to *n*-alcohol anesthetics on membrane mixing and antagonizes ethanol-induced anesthesia in a tadpole behavioral assay. Second, we show that two previously described "intoxication reversers" raise T_c and counter ethanol's effects in vesicles, mimicking the findings of previous electrophysiological and behavioral measurements. Third, we find that elevated hydrostatic pressure, long known to reverse anesthesia, also raises T_c in vesicles with a magnitude that counters the effect of butanol at relevant concentrations and pressures. Taken together, these results demonstrate that ΔT_c predicts anesthetic potency for *n*-alcohols better than hydrophobicity in a range of contexts, supporting a mechanistic role for membrane heterogeneity in general anesthesia.

INTRODUCTION

The potencies of many general anesthetics are roughly proportional to their oil-water partition coefficient over more than five orders of magnitude in overall concentration (1). This Meyer-Overton correlation suggests membrane involvement, and anesthetics have been shown to decrease lipid chain ordering, lower the main-chain melting temperature, and increase membrane spontaneous curvature, fluidity, and conductance (2–4). However, these effects are small (5) and often cannot account for those molecules that deviate from Meyer-Overton (6). Most recent attention focuses on the ion channels known to be most sensitive to these compounds (7), where extensive structural work (8–10) suggests that anesthetic effects are mediated by specific residues in hydrophobic membrane-spanning regions. High-potency general anesthetics such as etomidate and barbiturates are more effective at potentiating channels and producing anesthesia than predicted from their hydrophobicity alone, and evidence is accumulating that these compounds bind directly and specifically to channels at the interface between subunits (11).

Many researchers also favor a direct binding mechanism of anesthetic action for lower-potency anesthetics, including the *n*-alcohol anesthetics investigated here (8). However, channels are proposed to contain more numerous binding sites for these compounds (11–13), each with low affinity, leaving open the possibility that these anesthetics interact with channels more as solvents than as ligands.

Our understanding of the structure and function of the animal plasma membrane has grown dramatically since most membrane theories of anesthesia were put forward. It is now appreciated that animal plasma membranes have a thermodynamic tendency to separate into coexisting liquid domains, sometimes referred to as lipid rafts or lipid shells (14,15), and that this heterogeneity localizes and regulates ion channels, sometimes in a subtype-specific manner (16). Much of this regulation likely arises from the membrane's unusual thermodynamic properties. Cholesterol-containing membranes of purified lipids can support two distinct liquid phases (17), and giant plasma membrane vesicles (GPMVs) isolated from mammalian cell lines display analogous phase coexistence at low temperature (18). Remarkably, GPMVs are near the critical point of this transition (19), a nongeneric region of phase space distinguished by large correlation times and large but finite domain sizes

that requires fine tuning of both composition and temperature in synthetic systems (20).

We recently found (21) that incubating several general anesthetics with isolated GPMVs lowered their critical temperatures (T_c) in a way that scales well with their anesthetic dose as previously measured in tadpole loss-of-righting-reflex (LRR) assays (22). While our assay measures a change in T_c somewhat below the growth temperature, we predict that at higher temperatures, these treatments would destabilize submicron liquid domains both in vesicles and in the intact plasma membranes from which they were derived. Although this suggests a link between ΔT_c and anesthetic potency, we wanted to rule out the possibility that our observed correlation is derivative of a more fundamental correlation of both ΔT_c and anesthetic potency with hydrophobicity. As a first step toward this, we demonstrated that two hydrophobic but nonanesthetic analogs of general anesthetics did not affect T_c at concentrations at which Meyer-Overton predicts they would (21). Here, we explore a more direct challenge to the connection between changes in T_c and anesthetic potency by investigating the anesthetic effects of hydrophobic compounds and conditions that *raise* transition temperatures in GPMVs.

MATERIALS AND METHODS

GPMV measurements

Rat basal leukemia (RBL)-2H3 cells (23) were maintained in minimum essential media with 20% fetal bovine serum and 0.1% gentamicin at 37°C in 5% CO_2. XTC-2 cells (24) were maintained in L-15 media diluted 1:1.5 with water for amphibian cells with 10% fetal bovine serum, sodium bicarbonate (2.47 g/L), pen strep (100 units/mL) at room temperature in 5% CO_2. Freshly seeded cells were incubated in complete media for at least 18 h at the growth temperature indicated before GPMV isolation. All culture reagents were purchased from Thermo Fisher Scientific (Waltham, MA). Other reagents were purchased from Sigma Aldrich (St. Louis, MO) at the highest available purity unless otherwise indicated.

GPMVs from RBL cells were prepared through incubation with low concentrations of dithiothreitol (DTT, 2 mM) and formaldehyde (25 mM) in the presence of calcium (2 mM) for 1 h, as described previously (21). GPMVs isolated from RBL cells contain 20–40 mol % cholesterol, sphingolipids, phospholipids, and gangliosides typically associated with the plasma membrane, along with many transmembrane and peripheral plasma membrane proteins (18,25,26). For XTC-2-derived GPMVs, the vesiculation buffer was diluted 1:5 while maintaining calcium, formaldehyde, and DTT concentrations, and cells were incubated for at least 2 h at room temperature. Before GPMV formation, cells were labeled with DiI-C12 (Life Technologies, Carlsbad, CA; 2 μg/mL in 1% methanol) for 10 min at room temperature. GPMVs probed at atmospheric pressure were imaged on an inverted microscope (IX81; Olympus, Center Valley, PA) with a 40× air objective (0.95 NA), and epi-illumination using an Hg lamp and Cy3 filter set (Chroma Technology, Bellows Falls, VT). Temperature was controlled using a home-built Peltier stage, described previously (21), coupled to a proportional-integral-derivative controller (Oven Industries, Mechanicsburg, PA), and images were recorded using an sCMOS camera (Neo; Andor, South Windsor, CT).

GPMV suspensions with hexadecanol were prepared using either supersaturated solutions or equilibrated solutions. To make supersaturated solutions, hexadecanol was suspended in either dimethylsulfoxide (DMSO) or ethanol using volumes corresponding to the final concentrations indicated in the figures, then mixed directly with the GPMV suspension in aqueous buffer while mixing. The maximum DMSO concentration used was 0.5% v/v, and previous work demonstrates that T_c is not affected by DMSO treatment alone (21). Equilibrated solutions were prepared by first adding a concentrated hexadecanol stock directly to the GPMV suspension such that it precipitated out of solution. Then, the desired volume of ethanol was added and the solution mixed to facilitate the resuspension of hexadecanol. In all cases where ethanol and hexadecanol were added in combination, they were maintained at a 120 mM ethanol to 30 μM hexadecanol ratio, as indicated in figures. Equilibrated solutions could be made for 60 mM:1.5 μM, 120 mM:3 μM, 180 mM:4.5 μM, and 240 mM:6 μM (ethanol/hexadecanol ratio), although for higher concentrations some small fraction of hexadecanol lacked solubility. Only supersaturated solutions could be made for 600 mM:15 μM ethanol/hexadecanol.

Measurements conducted at elevated hydrostatic pressures were made using a custom-built microscopy-compatible pressure cell mounted on a Nikon Eclipse TE2000-E inverted microscope as described previously (27,28) with a 20× extra-long-working-distance air objective (0.4 NA) and G2-A filter set (Nikon Instruments, Richmond, UK) The pressure cell temperature was controlled via a circulating water bath. Images were acquired using an sCMOS based camera (Zyla; Andor, Belfast, United Kingdom) and recorded using custom-built software with temperature and pressure logging.

GPMV transition temperatures at constant pressure were measured as described previously (21) and as illustrated in Fig. 1 A. Briefly, images were acquired of fields of GPMVs over a range of temperatures such that at least 100 vesicles were detected at each temperature. After imaging, individual vesicles were identified as having a single liquid phase or two coexisting liquid phases. This information was compiled into a plot showing the percentage of vesicles with two liquid phases as a function of temperature, which was fit to a sigmoid function to extrapolate the temperature at which 50% of vesicles contained two coexisting liquid phases, % phase separated $= 100 \times (1 - 1/(1 + e^{-(T-T_c)/B}))$, where B is a parameter describing the width of the transition. The width of the transition within a population of vesicles ($\sim 10°C$) is much broader than the width of the transition for a single GPMV ($<2°C$) (19), most likely due to heterogeniety in composition between GPMVs (29).

We have previously demonstrated that these GPMVs pass through a critical temperature at the transition, even in the presence of anesthetics. Therefore, we refer to this temperature as the average critical temperature (T_c) of the sample. Errors in single measurements of T_c (σ_{T_c}) are 68% confidence-interval estimates of this parameter determined directly from the fit. For the example shown in Fig. 1 A, the T_c is 19.5 ± 0.6°C. We generally observe that average critical temperatures measured in this way vary in the range $12°C < T_c < 27°C$ for untreated RBL-derived GPMVs prepared as described above, depending on the growth conditions of the cells from which the GPMVs were derived (29). XTC-2 cells produced GPMVs with average critical temperatures of 14.8 ± 0.4° and 20.7 ± 0.4°C. Error bounds for a transition temperature shift (ΔT_c) are given by $\sqrt{\sigma_M^2 + \sigma_C^2}$, where σ_C is the error in measuring the T_c of the untreated control and σ_M is the error in measuring the T_c of the treated sample. The average critical pressure in the sample (P_c) at constant temperature was determined by a similar procedure, as illustrated in Fig. 1 B, although fit to a slightly different equation, % phase separated $= 100 \times (1/(1 + e^{-(P-P_c)/B}))$. As with previous studies in which only temperature was varied (19), we find that the fraction of phase-separated vesicles present in a population of vesicles at a given temperature/pressure does not depend on the order in which temperatures or pressures are sampled, suggesting that the transition is fully reversible.

Tadpole LRR measurements

Studies with *Xenopus laevis* tadpoles were conducted in compliance with the U.S. Department of Health and Human Services Guide for the Care and Use of Laboratory Animals and were approved by the University of Michigan Institutional Animal Care and Use Committee. *X. laevis* embryos were collected, fertilized, and dejellied as described previously (30).
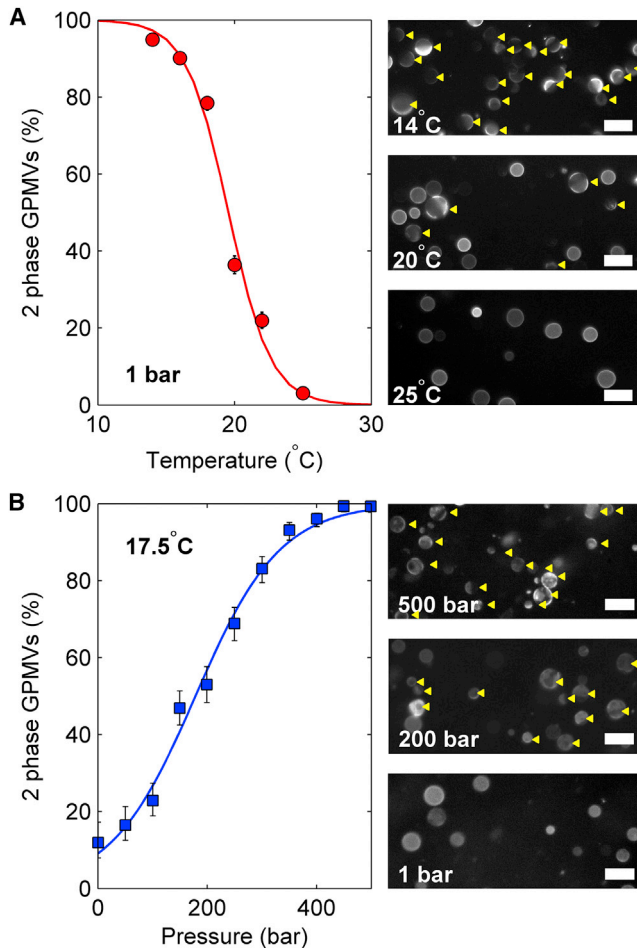
FIGURE 1 Determination of the average critical temperature or pressure of DiIC$_{12}$-labeled GPMVs through fluorescence imaging. (A) Fields containing multiple GPMVs were imaged over a range of temperatures and at fixed pressure, with representative subsets of images shown on the right. At high temperatures, most GPMVs appear uniform, whereas an increasing fraction of vesicles appear phase separated as the temperature is lowered, with phase-separated vesicles indicated by yellow arrows. From these images, we manually tabulate the fraction of GPMVs that contain two coexisting liquid phases as a function of temperature, constructing the plot on the left. These points are fit to the sigmoid function described in Materials and Methods to determine the extrapolated temperature at which 50% of vesicles contain coexisting liquid phases. (B) Fields containing multiple GPMVs were imaged over a range of pressures at fixed temperature, and representative subsets of images are shown on the right. At low pressure, most GPMVs appear uniform, whereas an increasing fraction of vesicles appear phase separated as pressure is increased. As with the fixed-pressure data in (A), these points are fit to the sigmoid function described in Materials and Methods to determine the extrapolated pressure at which 50% of vesicles contain coexisting liquid phases. To see this figure in color, go online.

Embryos were stored at room temperature in 0.1× MMR (Marc's Modified Ringers) (1× MMR = 100 mM NaCl, 2 mM KCl, 2 mM CaCl$_2$, 1 mM MgCl$_2$, and 5 mM Hepes, pH 7.4) and allowed to develop to the swimming-tadpole stage (stages 43–45).

The LRR response was determined by placing tadpoles in a clean glass container filled with 50 mL filtered well water (the same water used to house adult frogs) and the specified concentration of n-alcohols. At 10 min intervals, tadpoles were probed with a smooth glass rod and their

responses recorded. Measurements with ethanol or ethanol and hexadecanol in equilibrated solutions were conducted on three separate occasions, each time with five tadpoles per condition, for a total of 15 tadpoles per condition. Some measurements were conducted double-blind to avoid possible systematic bias in the behavioral scoring. Fewer tadpoles were probed for the other n-alcohol combinations investigated. Error bars on LRR measurements are 68% confidence intervals with binomial errors calculated according to $LB = 1 - \beta Inv(0.32/2, n - nk, nk + 1)$ and $UB = 1 - \beta Inv(1 - 0.32/2, n - nk + 1, nk)$, where LB and UB are the lower and upper bounds of the confidence interval, respectively, n is the number of tadpoles investigated, k is the fractional LRR, and βInv is the β-inverse cumulative distribution function.

To estimate the concentration at which 50% of tadpoles are anesthetized (AC$_{50}$), LRR measurements at a range of ethanol concentrations were fit to the form $LRR = 1 - (1/1 + e^{-([EtOH]-AC50)/B})$. Errors reported are 68% confidence intervals of parametric uncertainty in AC$_{50}$. These are calculated by inverting the expectation value of the Fisher information and then taking the square root of its diagonal entry. Error bars are much larger for hexadecanol-containing titrations, because all data are taken below the extrapolated AC$_{50}$.

RESULTS

Fig. 2 A shows that incubating supersaturated solutions of hexadecanol (n = 16 alcohol) with isolated RBL- and XTC-2-derived GPMVs acts to raise T_c. Here, GPMVs derived from both mammalian (RBL) and *X. laevis* (XTC-2) cells were used to demonstrate robustness of this effect across species, since later measurements are conducted in *X. laevis* tadpoles. The sign change in ΔT_c for hexadecanol compared to shorter-chain n-alcohols mirrors past work in which it was found that hexadecanol acted to increase chain order within native isolated membranes, whereas shorter anesthetic n-alcohols acted to decrease chain order (31). We
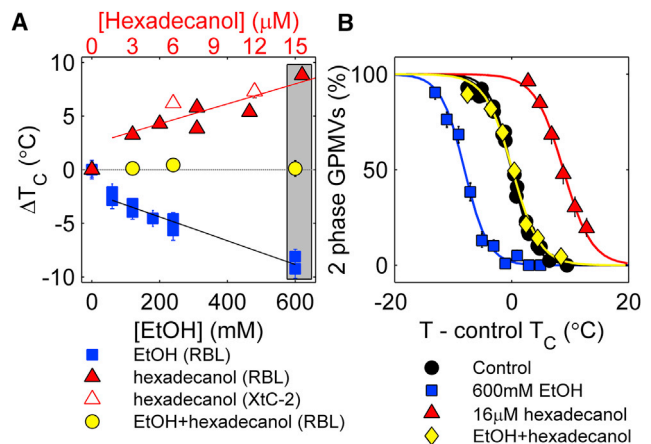
FIGURE 2 Hexadecanol raises T_c in GPMVs from rat (RBL) and *Xenopus* (XTC-2) cell lines and can counteract the T_c-lowering effects of ethanol. (A) Values indicate the average shift in T_c (ΔT_c) in a population of vesicles upon treatment with the compounds indicated. Solutions containing hexadecanol were prepared to be supersaturated, as described in Materials and Methods. Each point represents a single measurement, and error bounds represent the 68% confidence interval on the extrapolated ΔT_c. (B) Plots showing the fraction of phase-separated vesicles versus temperature for the three points inside the gray box in (A). To see this figure in color, go online.

find that the effect on ΔT_c is approximately additive when ethanol ($n = 2$ alcohol) and hexadecanol are used in combination, with 3 μM hexadecanol required to counter the effect of an AC_{50} of ethanol (120 mM) over a range of ethanol and hexadecanol concentrations (Fig. 2, A and B).

Mimicking results from our previous study with n-alcohols (21), we again find that relatively small concentrations of both hexadecanol and ethanol lead to a steep change in ΔT_c, whereas larger concentrations lead to a less steep and approximately linear regime. This nonlinearity implies an interaction between the added molecules, but we cannot specify the nature of their interaction from our measurements. It could be that the concentration of n-alcohol in the membrane becomes a sublinear function of the concentration of these n-alcohols in the bulk. Past work has demonstrated that n-alcohol membrane partition coefficients can depend on n-alcohol concentration (32), membrane composition (32,33), and temperature (33), and it is possible that these or related effects could lead to the observed nonlinearity. Another possibility is that the addition of small molecules could increase the area of the membrane, thereby reducing its tension. This could have a direct effect on T_c (34) or could alter the membrane's affinity for additional small molecules. It is also possible that membrane concentration is linear with that of the bulk, but that T_c is a nonlinear function of n-alcohol concentration in the membrane. We note that ethanol can induce a novel interdigitated membrane phase in purified phosphatidylcholine membranes at high enough concentrations (35,36), so it is plausible that specific interactions between certain lipids and alcohols could drive at least some of the nonlinearity that we observe. At AC_{50}, small molecules make up several mol % of the membrane (22), a relatively high concentration that makes it plausible that n-alcohols interact directly, or indirectly, through membrane-mediated mechanisms that can be very sensitive near the critical point (37).

Our observation that hexadecanol can counteract the effects of ethanol in GPMVs led us to speculate that hexadecanol could antagonize ethanol anesthesia. To test this hypothesis, we examined the tadpole LRR in *X. laevis* tadpoles (Fig. 3 A). We also measured the extent to which identical n-alcohol treatments alter T_c in RBL-derived GPMVs. Here, equilibrated solutions of hexadecanol and ethanol were used, leading to small differences from the results presented in Fig. 2. In ethanol alone, 50% of tadpoles did not exhibit a righting reflex upon inverting with a glass rod at 118 ± 15 mM ethanol, in agreement with previous reports of 120 mM (22). Tadpoles incubated in ethanol and
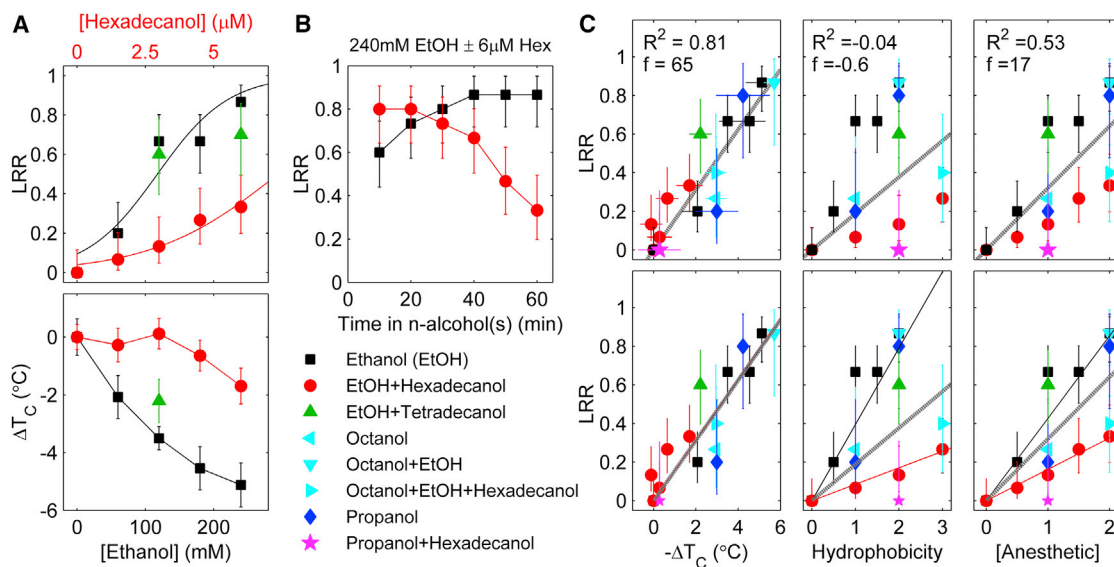

FIGURE 3 (A) (*Upper*) Tadpole LRR for a titration of ethanol alone and combinations of ethanol and hexadecanol (EtOH+Hex) or ethanol and tetradecanol (EtOH+Tet) measured after 1 h incubation in equilibrated solutions. At a given ethanol concentration, the fraction of tadpoles that respond to stimulus increases in the presence of hexadecanol (EtOH+Hex; *red circles, upper horizontal axis*). The EtOH+Tet combination contains either 5 or 10 μM tetradecanol (*green triangles*). (*Lower*) ΔT_c in RBL-derived GPMVs is shown for identical titrations. All solutions contain the ethanol concentration indicated by the lower horizontal axis. (B) Time course of LRR for one ethanol and EtOH+Hex combination. (C) (*Left*) Points in (A) replotted as LRR versus ΔT_c, including additional experiments with other n-alcohol combinations, as indicated in the legend. (*Center*) LRR plotted versus aggregate hydrophobicity, tabulated by summing the concentration of each n-alcohol present normalized by its AC_{50} (22), using 3 μM as a proxy AC_{50} for hexadecanol and 5 μM as a proxy AC_{50} for tetradecanol. (*Right*) LRR plotted versus the net anesthetic concentration, tabulated by summing the concentration of each $n < 14$ alcohol anesthetic present normalized by its AC_{50} (22). (*Top row*) In each case, the dashed line represents a best fit to the data, with R^2 values giving the fraction of explained variance and f values comparing the quality of the fit to a null model where all points have the same probability. All fits are linear and constrained to go through the origin. (*Bottom row*) In each case, the black line is fit to all conditions that exclude hexadecanol, the red line is fit to all conditions that include hexadecanol, and the gray dashed line is fit to all points, as in the top row. These fits are substantially different from each other, except when plotted versus ΔT_c, indicating that ΔT_c has the most quantitative predictive power across chemical species. To see this figure in color, go online.

hexadecanol remained alert to much higher ethanol concentrations, more than doubling the extrapolated AC_{50} value to 294 ± 61 mM. Coincubation with tetradecanol ($n = 14$) had little effect either on GPMV transition temperatures or on the tadpole LRR, suggesting that competitive inhibition at a putative ethanol binding site is not the mechanism through which hexadecanol reverses the effects of ethanol on LRR.

Fig. 3 B shows the time-dependent effects of ethanol and ethanol-hexadecanol mixtures on tadpole LRRs. LRR is not initially affected by the presence of hexadecanol, but instead is reduced over the span of 1 h compared to LRRs incubated in ethanol alone. Experiments were not extended beyond 1 h, as we observed some adaptation of ethanol-treated tadpoles beyond this time frame. The slow onset of hexadecanol action is consistent with past work using radiolabeled n-alcohols, which demonstrated that their absorption dynamics depend on carbon length, with longer n-alcohols requiring longer times for incorporation (31). We note that the apparent difference in LRR for ethanol+hexadecanol versus ethanol alone is not significant at early time points, nor is the apparent upward trend in LRR versus time for tadpoles treated with ethanol alone.

In Fig. 3 C, we plot LRR versus ΔT_c, aggregate hydrophobicity, and anesthetic concentration for a range of conditions. We find that ΔT_c captures substantially more of the variance in LRR across trials ($R^2 = 0.82$) compared to summed anesthetic potency ($R^2 = 0.53$), whereas aggregate hydrophobicity has no predictive power ($R < 0$). This is partially due to our carefully chosen treatments, many of which are hydrophobic but raise critical temperatures and antagonize LRR. Furthermore, we find that ΔT_c predicts LRR with the same function whether for treatments with or treatments without hexadecanol, whereas both aggregate hydrophobicity and summed anesthetic potency do not. Together this demonstrates that ΔT_c predicts LRR across molecular species.

The extremely low solubility of hexadecanol presents some experimental difficulties. Ethanol is required as a co-solvent in these measurements, and this prevented a more systematic exploration of how hexadecanol modulates anesthesia mediated by other n-alcohols and anesthetics. Our reliance on ethanol as a general anesthetic introduces technical challenges, since it has low potency, can harbor impurities that modulate LRR measurements (31), and produces alternate functional outcomes when used at high concentrations (38). Although a more water-soluble T_c-raising compound would alleviate some of these problems, most membrane-soluble molecules with reasonable water solubility either lower GPMV transition temperatures or leave them unchanged. Notable exceptions are some detergents (39), which are not suitable for this investigation because they also permeabilize membranes. Molecules that raise T_c must partition more strongly than the average component into one low-temperature membrane phase (40) and our observations suggest that this often requires a large hydrophobic interaction area, with consequent low solubility in water.

Two other compounds are reported to reverse the intoxicating effects of ethanol in both cultured neurons and intact organisms, and their effects on RBL-derived GPMVs are shown in Fig. 4. A therapeutic agent, RO15-4513 (100 nM), used to reverse acute ethanol toxicity, has been demonstrated to reverse effects of 30 mM ethanol in the GABA current in oocytes (41). We find that 100 nM RO15-4513 raises critical temperatures in GPMVs by $1.2 \pm 0.4°C$. Similarly, 3 μM dihydromyricetin was recently reported to antagonize the effects of 60 mM ethanol on the GABA-induced current in acutely dissociated rat hippocampal slices as well as in behavioral assays in vivo (42). We find that 3 μM dihydromyricetin raises critical temperatures by $1.3 \pm 0.5°C$. In each of these cases, the effect of these compounds on T_c appears to saturate at concentrations well below their solubility. Although we have no mechanistic explanation for this saturation, we note that it is mirrored in past behavioral measurements (41,42) showing that DHM and RO15-4513 are only able to counter ethanol effects to concentrations well below its AC_{50} of 120 mM.

Although the correlation between ΔT_c and anesthetic function is robust for the compounds investigated, we note that an additional compound, menthol, raises T_c by nearly 2°C when added to RBL-derived GPMVs at 100 μM (43), yet acts as an anesthetic in tadpole LRR measurements at somewhat lower concentrations ($AC_{50} \approx 20$ μM) (44). This could be due to menthol having specific interactions with $GABA_A$ receptors, as has been proposed previously (44). It is also possible that menthol has different effects on *X. laevis* neuronal versus mammalian immune plasma membranes.

We also investigated the effects of hydrostatic pressure on GPMVs in the presence and absence of butanol ($n = 4$ alcohol). It has long been known that 150–200 bar of pressure reverses animal anesthesia (45). Here, we show that the fraction of vesicles with two-phase coexistence increases monotonically with pressure for vesicles incubated with and without butanol (Fig. 5 A). We observe that 240 ± 30 bar is needed to counter the effects of one AC_{50} of
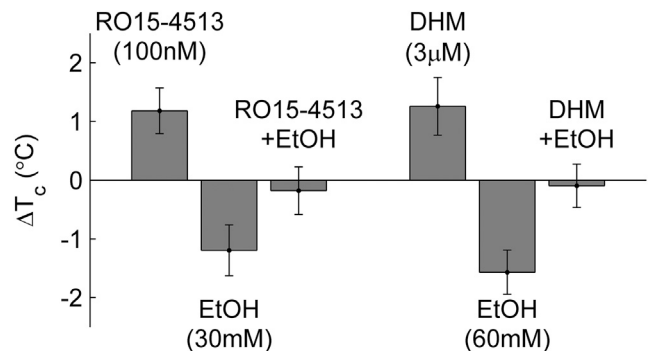

FIGURE 4 RO15-4513 and dihydromyricetin block the acute toxicity and intoxicating effect of ethanol. Each raises T_c and cancels the effects of ethanol when added to GPMVs at the same concentration at which they are effective in vivo.
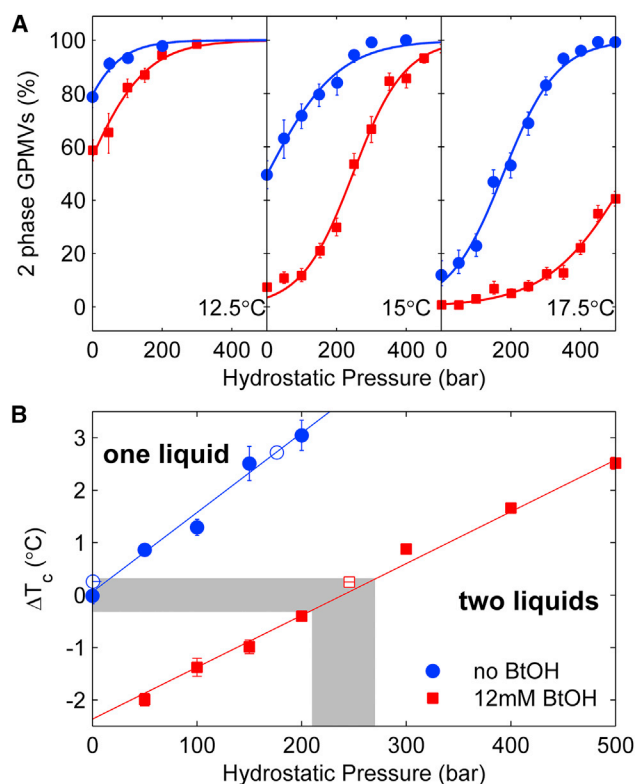
FIGURE 5 (A) The fraction of vesicles that are macroscopically phase separated is plotted as a function of hydrostatic pressure at three different temperatures for both control vesicles and vesicles incubated with 12 mM butanol (BtOH). In each case, increasing the pressure leads to an increase in the fraction of vesicles that are macroscopically phase separated. (B) T_c rises with increasing hydrostatic pressure in both control GPMVs and GPMVs incubated in BtOH. Here, 240 ± 30 bar of hydrostatic pressure is required to reverse the effects of 12 mM BtOH (shaded region). Solid symbols are obtained by extrapolating to find T_c from the data acquired at constant pressure, whereas open symbols are obtained by extrapolating to find P_c at constant temperature. At temperatures above T_c, most vesicles are composed of a macroscopically uniform single liquid, whereas below T_c, most are separated into two coexisting liquid phases. To see this figure in color, go online.

butanol (12 mM (22)) on the T_c of RBL-derived GPMVs (Fig. 5 B). Pressure reversal of general anesthesia is not accounted for by current models involving direct binding of anesthetics to channels, because protein conformational equilibria are typically sensitive only to much larger pressures (>1000 bar) (46,47). These smaller pressures can have large effects on some membrane properties, and past work has shown that 200 bar raises the main-chain melting temperature in synthetic single-component lipid systems by ~ 4.5°C (48,49), even more than is observed here for the miscibility transition in GPMVs (2–3°C).

DISCUSSION

Although our results are not sufficient to specify a mechanism, they do strongly suggest that n-alcohol anesthetic inhibition of membrane heterogeneity plays an important role

in mediating anesthesia, likely by interfering with normal membrane regulation of ion channels. We have previously argued that the presence of a critical point in GPMVs near or below room temperature leads to extended and dynamic composition fluctuations at growth temperature (typically 37°C), both in isolated vesicles and in the intact plasma membranes from which they are derived (19,50). Theory and experiment suggest that the size of fluctuations varies as $(T - T_c)^{-1}$ (19,51), so that lowering T_c through the addition of an n-alcohol anesthetic is expected to reduce the size of compositional heterogeneity at a fixed growth temperature (Fig. 6). This suggests several plausible mechanisms through which changes in plasma membrane T_c could modulate channel function. First, reducing the size of membrane structures could in principle increase (or decrease) accessibility of native regulators of channel function such as neurosteroids, phosphoinositides, and G-proteins (16). Second, different membrane domains are expected to differ
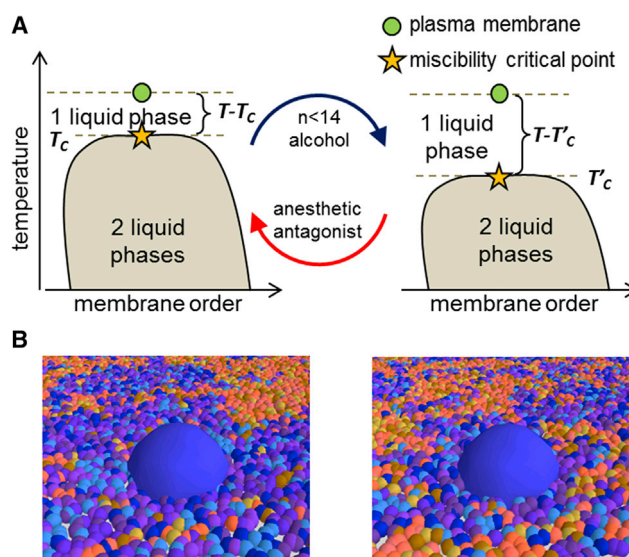

FIGURE 6 Anesthetics lower the transition temperature of a biologically tuned critical point, which could lead to misregulation of ion channels and other membrane-bound proteins. (A) Schematic phase diagrams for the plasma membrane of an untreated and an n-alcohol-treated cell. Guided by experiments (19), we hypothesize that the plasma membrane lies in the white region where lipids, proteins, and other membrane components are well mixed macroscopically into a single two-dimensional liquid phase. However, due to their close proximity to the critical point (star), thermal fluctuations lead to relatively large domains enriched in particular components. When cooled into the gray two-phase region, GPMVs separate into two coexisting liquid phases termed liquid-ordered and liquid-disordered. Several n-alcohol general anesthetics lower the critical temperature of the membrane (21), changing the distance above the critical point, $T - T_c$. Here, we also show that treatments that antagonize anesthetic action raise critical temperatures, reversing the effects of n-alcohols on T_c. (B) Under normal conditions, a hypothetical ion channel (large blue inclusion) has a tendency to inhabit relatively large domains enriched in particular lipids and proteins. When the membrane is taken away from the critical point, the structure of these domains is altered, possibly leading to changes in ion channel gating and function through a variety of mechanisms discussed in the text. To see this figure in color, go online.

in physical properties such as hydrophobic thickness, lateral pressure profiles, viscosity, and bending rigidity (52–56). Destabilizing these membrane domains could act to modulate the response of channels directly by stabilizing different internal protein states. Third, membrane domains are argued to play important roles in organizing channels at neuronal synapses (16) and destabilizing these domains could lead to altered localization of channels with disruption of higher-level neuronal functions. Each of these mechanistic possibilities has a distinct experimental signature that can be explored in future studies.

One naive prediction of our model is not borne out by experiment, namely that the functional effects of anesthetics are not readily reversed by lowering ambient temperature (57), even though this should reverse anesthetic effects on the parameter $T - T_c$. Although this finding is at odds with a simple interpretation of our results, we note that other biological functions have been shown to be explicitly temperature compensated (58,59). In these examples, individual reaction rates often display sharp temperature sensitivity, but the effects of these changes on certain important axes (e.g., the timing of the circadian clock) roughly cancel, leaving function robust (60). Thus, although many cellular processes relevant to neuronal function have sensitive temperature dependence (61–63), we expect that organisms, especially those able to live over a range of temperatures, have evolved to a regime where neural function is temperature compensated (63) and is thus surprisingly insensitive to changes in temperature. However, we might still expect that triggering only the effects of temperature on membrane criticality in an uncompensated way, as we argue occurs with n-alcohol anesthesia, might lead to dramatic changes in function (60). We note that in some past studies, behavioral measurements in temperature-adapted animals were conducted (64,65) that demonstrated a lack of temperature dependence on anesthetic potency, whereas other studies have found evidence for concurrent changes in membrane composition (66,67). Acute temperature changes mimicking or exceeding those produced by relevant concentrations of anesthetic ($\pm 4°C$) do produce behavioral changes in animals, ranging from lethargy to death (64).

Finally, although the evidence for anesthetic-channel interactions is significant, several features may suggest that the interaction is more akin to two-dimensional solvent-solute rather than binding-site-ligand interactions. Some channels contain multiple proposed binding sites for low-potency anesthetics, each with low-affinity but diffusion-limited association rates (12), with clinically relevant concentrations of anesthetic as high as several mol % of the membrane (68). Additionally, many anesthetic-sensitive channels are also sensitive to membrane properties, in particular cholesterol modulation, in both reconstituted (69) and cellular systems (70), suggesting a commonality with broader regulation by membrane domains. Our results suggest that these effects on channel function are likely to be altered by anesthetics through their effects on membrane mixing, even without binding of anesthetic to protein targets.

CONCLUSIONS

Overall, the results presented here demonstrate that a condition's effect on the GPMV T_c is more predictive of anesthetic potency than of hydrophobicity. By exploiting rare conditions where $\Delta T_c > 0$ we have shown that behavioral measures and existing electrophysiological assays for anesthesia are remarkably tied to the membrane's thermodynamic propensity to form small domains. Although our results do not suggest a specific mechanism through which these conditions reverse the effects of anesthesia, they do support the hypothesis that at least some n-alcohol targets are influenced through effects on membrane criticality.

AUTHOR CONTRIBUTIONS

GPMV experiments were carried out by E.G., E.M.G., M.N., and S.L.V. in the lab of S.L.V. Tadpole experiments were carried out by E.G., E.M.G., B.B.M., A.L.M., M.N., and S.L.V. in the lab of A.L.M. Experiments at high pressure were carried out by N.J.B., N.L.C.M., and S.L.V. in the lab of N.J.B. S.L.V. analyzed the data, N.J.B., B.B.M., A.L.M., and S.L.V. designed the research, and B.B.M. and S.L.V. wrote the article.

ACKNOWLEDGMENTS

REFERENCES

1. Meyer, H. 1899. Zur theorie der alkoholnarkose. *Arch. Exp. Path. Pharm.* 42:109–118.

2. Gruner, S. M., and E. Shyamsunder. 1991. Is the mechanism of general anesthesia related to lipid membrane spontaneous curvature? *Ann. N. Y. Acad. Sci.* 625:685–697.

3. Wodzinska, K., A. Blicher, and T. Heimburg. 2009. The thermodynamics of lipid ion channel formation in the absence and presence of anesthetics. BLM experiments and simulations. *Soft Matter.* 5:3319–3330.

4. Ingólfsson, H. I., and O. S. Andersen. 2011. Alcohol's effects on lipid bilayer properties. *Biophys. J.* 101:847–855.

5. Herold, K. F., R. L. Sanford, …, H. C. Hemmings, Jr. 2014. Volatile anesthetics inhibit sodium channels without altering bulk lipid bilayer properties. *J. Gen. Physiol.* 144:545–560.

6. Franks, N. P., and W. R. Lieb. 1986. Partitioning of long-chain alcohols into lipid bilayers: implications for mechanisms of general anesthesia. *Proc. Natl. Acad. Sci. USA.* 83:5116–5120.

7. Franks, N. P., and W. R. Lieb. 1994. Molecular and cellular mechanisms of general anaesthesia. *Nature*. 367:607–614.

8. Mihic, S. J., Q. Ye, …, N. L. Harrison. 1997. Sites of alcohol and volatile anaesthetic action on GABA(A) and glycine receptors. *Nature*. 389:385–389.

9. Borghese, C. M., D. F. Werner, …, N. L. Harrison. 2006. An isoflurane- and alcohol-insensitive mutant GABA$_A$ receptor α_1 subunit with near-normal apparent affinity for GABA: characterization in heterologous systems and production of knockin mice. *J. Pharmacol. Exp. Ther.* 319:208–218.

10. Nury, H., C. Van Renterghem, …, P. J. Corringer. 2011. X-ray structures of general anaesthetics bound to a pentameric ligand-gated ion channel. *Nature*. 469:428–431.

11. Forman, S. A., and K. W. Miller. 2016. Mapping general anesthetic sites in heteromeric γ-aminobutyric acid type A receptors reveals a potential ror targeting receptor subtypes. *Anesth. Analg.*, in press.

12. Xu, Y., T. Seto, …, L. Firestone. 2000. NMR study of volatile anesthetic binding to nicotinic acetylcholine receptors. *Biophys. J.* 78:746–751.

13. Brannigan, G., D. N. LeBard, …, M. L. Klein. 2010. Multiple binding sites for the general anesthetic isoflurane identified in the nicotinic acetylcholine receptor transmembrane domain. *Proc. Natl. Acad. Sci. USA*. 107:14122–14127.

14. Simons, K., and E. Ikonen. 1997. Functional rafts in cell membranes. *Nature*. 387:569–572.

15. Anderson, R. G., and K. Jacobson. 2002. A role for lipid shells in targeting proteins to caveolae, rafts, and other lipid domains. *Science*. 296:1821–1825.

16. Allen, J. A., R. A. Halverson-Tamboli, and M. M. Rasenick. 2007. Lipid raft microdomains and neurotransmitter signalling. *Nat. Rev. Neurosci.* 8:128–140.

17. Veatch, S. L., and S. L. Keller. 2005. Seeing spots: Complex phase behavior in simple membranes. *Biochim. Biophys. Acta.* 1746:172–185.

18. Baumgart, T., A. T. Hammond, …, W. W. Webb. 2007. Large-scale fluid/fluid phase separation of proteins and lipids in giant plasma membrane vesicles. *Proc. Natl. Acad. Sci. USA*. 104:3165–3170.

19. Veatch, S. L., P. Cicuta, …, B. Baird. 2008. Critical fluctuations in plasma membrane vesicles. *ACS Chem. Biol.* 3:287–293.

20. Honerkamp-Smith, A. R., P. Cicuta, …, S. L. Keller. 2008. Line tensions, correlation lengths, and critical exponents in lipid membranes near critical points. *Biophys. J.* 95:236–246.

21. Gray, E., J. Karslake, …, S. L. Veatch. 2013. Liquid general anesthetics lower critical temperatures in plasma membrane vesicles. *Biophys. J.* 105:2751–2759.

22. Pringle, M. J., K. B. Brown, and K. W. Miller. 1981. Can the lipid theories of anesthesia account for the cutoff in anesthetic potency in homologous series of alcohols? *Mol. Pharmacol.* 19:49–55.

23. Barsumian, E. L., C. Isersky, …, R. P. Siraganian. 1981. IgE-induced histamine release from rat basophilic leukemia cell lines: isolation of releasing and nonreleasing clones. *Eur. J. Immunol.* 11:317–323.

24. Pudney, M., M. G. Varma, and C. J. Leake. 1973. Establishment of a cell line (XTC-2) from the South African clawed toad, *Xenopus laevis*. *Experientia*. 29:466–467.

25. Fridriksson, E. K., P. A. Shipkova, …, F. W. McLafferty. 1999. Quantitative analysis of phospholipids in functionally important membrane domains from RBL-2H3 mast cells using tandem high-resolution mass spectrometry. *Biochemistry*. 38:8056–8063.

26. Levental, K. R., J. H. Lorent, …, I. Levental. 2016. Polyunsaturated lipids regulate membrane domain stability by tuning membrane order. *Biophys. J.* 110:1800–1810.

27. McCarthy, N. L. C., O. Ces, …, N. J. Brooks. 2015. Separation of liquid domains in model membranes induced with high hydrostatic pressure. *Chem. Commun. (Camb.)*. 51:8675–8678.

28. Purushothaman, S., P. Cicuta, …, N. J. Brooks. 2015. Influence of high pressure on the bending rigidity of model membranes. *J. Phys. Chem. B.* 119:9805–9810.

29. Gray, E. M., G. Díaz-Vázquez, and S. L. Veatch. 2015. Growth conditions and ell ycle phase modulate phase transition temperatures in RBL-2H3 derived plasma membrane vesicles. *PLoS One*. 10:e0137741.

30. Miller, A. L., and W. M. Bement. 2009. Regulation of cytokinesis by Rho GTPase flux. *Nat. Cell Biol.* 11:71–77.

31. Miller, K. W., L. L. Firestone, …, P. Streicher. 1989. Nonanesthetic alcohols dissolve in synaptic membranes without perturbing their lipids. *Proc. Natl. Acad. Sci. USA*. 86:1084–1087.

32. Fraser, D. M., L. C. Van Gorkom, and A. Watts. 1991. Partitioning behaviour of 1-hexanol into lipid membranes as studied by deuterium NMR spectroscopy. *Biochim. Biophys. Acta.* 1069:53–60.

33. Trandum, C., P. Westh, …, O. G. Mouritsen. 2000. A thermodynamic study of the effects of cholesterol on the interaction between liposomes and ethanol. *Biophys. J.* 78:2486–2492.

34. Portet, T., S. E. Gordon, and S. L. Keller. 2012. Increasing membrane tension decreases miscibility temperatures; an experimental demonstration via micropipette aspiration. *Biophys. J.* 103:L35–L37.

35. Rowe, E. S., and T. A. Cutrera. 1990. Differential scanning calorimetric studies of ethanol interactions with distearoylphosphatidylcholine: transition to the interdigitated phase. *Biochemistry*. 29:10398–10404.

36. McIntosh, T. J., H. Lin, …, C. Huang. 2001. The effect of ethanol on the phase transition temperature and the phase structure of monounsaturated phosphatidylcholines. *Biochim. Biophys. Acta.* 1510:219–230.

37. Widom, B. 1967. Plait points in 2 and 3-component liquid mixtures. *J. Chem. Phys.* 46:3324–3333.

38. Downes, H., and P. M. Courogen. 1996. Contrasting effects of anesthetics in tadpole bioassays. *J. Pharmacol. Exp. Ther.* 278:284–296.

39. Zhou, Y., K. N. Maxwell, …, I. Levental. 2013. Bile acids modulate signaling by functional perturbation of plasma membrane domains. *J. Biol. Chem.* 288:35660–35670.

40. Meerschaert, R. L., and C. V. Kelly. 2015. Trace membrane additives affect lipid phases with distinct mechanisms: a modified Ising model. *Eur. Biophys. J.* 44:227–233.

41. Wallner, M., H. J. Hanchar, and R. W. Olsen. 2006. Low-dose alcohol actions on $\alpha_4\beta_3\delta$ GABA$_A$ receptors are reversed by the behavioral alcohol antagonist Ro15-4513. *Proc. Natl. Acad. Sci. USA*. 103:8540–8545.

42. Shen, Y., A. K. Lindemeyer, …, J. Liang. 2012. Dihydromyricetin as a novel anti-alcohol intoxication medication. *J. Neurosci.* 32:390–401.

43. Raghunathan, K., A. Ahsan, …, S. L. Veatch. 2015. Membrane transition temperature determines cisplatin response. *PLoS One*. 10:e0140925.

44. Watt, E. E., B. A. Betts, …, A. C. Hall. 2008. Menthol shares general anesthetic activity and sites of action on the GABA$_A$ receptor with the intravenous agent, propofol. *Eur. J. Pharmacol.* 590:120–126.

45. Johnson, F. H., and E. A. Flagler. 1950. Hydrostatic pressure reversal of narcosis in tadpoles. *Science*. 112:91–92.

46. Moss, G. W., W. R. Lieb, and N. P. Franks. 1991. Anesthetic inhibition of firefly luciferase, a protein model for general anesthesia, does not exhibit pressure reversal. *Biophys. J.* 60:1309–1314.

47. Mozhaev, V. V., K. Heremans, …, C. Balny. 1996. High pressure effects on protein structure and function. *Proteins*. 24:81–91.

48. Liu, N.-I., and R. L. Kay. 1977. Redetermination of the pressure dependence of the lipid bilayer phase transition. *Biochemistry*. 16:3484–3486.

49. Winter, R., and C. Jeworrek. 2009. Effect of pressure on membranes. *Soft Matter*. 5:3157–3173.

50. Machta, B. B., S. Papanikolaou, …, S. L. Veatch. 2011. Minimal model of plasma membrane heterogeneity requires coupling cortical actin to criticality. *Biophys. J.* 100:1668–1677.

51. Zhao, J., J. Wu, and S. L. Veatch. 2013. Adhesion stabilizes robust lipid heterogeneity in supercritical membranes at physiological temperature. *Biophys. J.* 104:825–834.

52. Diaz-Rohrer, B. B., K. R. Levental, …, I. Levental. 2014. Membrane raft association is a determinant of plasma membrane localization. *Proc. Natl. Acad. Sci. USA.* 111:8500–8505.

53. Lin, Q., and E. London. 2013. Altering hydrophobic sequence lengths shows that hydrophobic mismatch controls affinity for ordered lipid domains (rafts) in the multitransmembrane strand protein perfringolysin O. *J. Biol. Chem.* 288:1340–1352.

54. Niemelä, P. S., S. Ollila, …, I. Vattulainen. 2007. Assessing the nature of lipid raft membranes. *PLOS Comput. Biol.* 3:e34.

55. Cicuta, P., S. L. Keller, and S. L. Veatch. 2007. Diffusion of liquid domains in lipid bilayer membranes. *J. Phys. Chem. B*. 111:3328–3331.

56. Baumgart, T., S. T. Hess, and W. W. Webb. 2003. Imaging coexisting fluid domains in biomembrane models coupling curvature and line tension. *Nature*. 425:821–824.

57. Franks, N. P., and W. R. Lieb. 1982. Molecular mechanisms of general anaesthesia. *Nature*. 300:487–493.

58. Oleksiuk, O., V. Jakovljevic, …, V. Sourjik. 2011. Thermal robustness of signaling in bacterial chemotaxis. *Cell*. 145:312–321.

59. Kidd, P. B., M. W. Young, and E. D. Siggia. 2015. Temperature compensation and temperature sensation in the circadian clock. *Proc. Natl. Acad. Sci. USA.* 112:E6284–E6292.

60. Daniels, B. C., Y.-J. Chen, …, C. R. Myers. 2008. Sloppiness, robustness, and evolvability in systems biology. *Curr. Opin. Biotechnol.* 19:389–395.

61. Smith, S. M., R. Renden, and H. von Gersdorff. 2008. Synaptic vesicle endocytosis: fast and slow modes of membrane retrieval. *Trends Neurosci.* 31:559–568.

62. Thompson, S. M., L. M. Masukawa, and D. A. Prince. 1985. Temperature dependence of intrinsic membrane properties and synaptic potentials in hippocampal CA1 neurons in vitro. *J. Neurosci.* 5:817–824.

63. Tang, L. S., M. L. Goeritz, …, E. Marder. 2010. Precise temperature compensation of phase in a rhythmic motor pattern. *PLoS Biol.* 8:1–13.

64. Meyer, H. 1901. Zur theorie der alkoholnarkose. 3. Mittheilung: der einfluss wechselnder temperatur auf wirkungsstrke und theilungscoefficient der narcotiea. *Arch. Exp. Path. Pharm.* 46:338346.

65. Cherkin, A., and J. F. Catchpool. 1964. Temperature dependence of anesthesia in goldfish. *Science*. 144:1460–1462.

66. Barańska, J., and P. Wlodawer. 1969. Influence of temperature on the composition of fatty acids and on lipogenesis in frog tissues. *Comp. Biochem. Physiol.* 28:553–570.

67. Anderson, T. R. 1970. Temperature adaptation and the phospholipids of membranes in goldfish (*Carassius auratus*). *Comp. Biochem. Physiol.* 33:663–687.

68. Janoff, A. S., M. J. Pringle, and K. W. Miller. 1981. Correlation of general anesthetic potency with solubility in membranes. *Biochim. Biophys. Acta.* 649:125–128.

69. Bristow, D. R., and I. L. Martin. 1987. Solubilisation of the γ-aminobutyric acid/benzodiazepine receptor from rat cerebellum: optimal preservation of the modulatory responses by natural brain lipids. *J. Neurochem.* 49:1386–1393.

70. Sooksawate, T., and M. A. Simmonds. 2001. Effects of membrane cholesterol on the sensitivity of the $GABA_A$ receptor to GABA in acutely dissociated rat hippocampal neurones. *Neuropharmacology*. 40:178–184.